
GOAL-ORIENTED TIME-SERIES FORECASTING: FOUNDATION FRAMEWORK DESIGN

Luca-Andrei Fechete^{*†} Mohamed Sana[†] Fadhel Ayed[†] Nicola Piovesan[†] Wenjie Li[†]
Antonio De Domenico[†] Tareq Si Salem[‡]

June 7, 2025

ABSTRACT

Traditional time-series forecasting often focuses only on minimizing prediction errors, ignoring the specific requirements of real-world applications that employ them. This paper presents a new training methodology, which allows a forecasting model to dynamically adjust its focus based on the importance of forecast ranges specified by the end application. Unlike previous methods that fix these ranges beforehand, our training approach breaks down predictions over the entire signal range into smaller segments, which are then dynamically weighted and combined to produce accurate forecasts within a region of interest. We tested our method on standard datasets, including a new wireless communication dataset, and found that not only it improves prediction accuracy but also enhances the performance of end application employing the forecasting model. This research provides a basis for creating forecasting systems that better connect prediction and decision-making in various practical applications.

^{*}École Polytechnique, Palaiseau, France (Research Intern)

[†]Paris Research Center, Huawei Technologies, Boulogne-Billancourt, France

[‡]Lead researcher for this study. Corresponding author: tareq.si.salem@huawei.com

1 Introduction

Time-series forecasting (TSF) represents a significant area of study within machine learning (ML), with practical applications demonstrable in various domains, including but not limited to, economics [15], energy resource management [26, 31], transportation optimization [7], meteorological prediction [40], inventory optimization [20], and healthcare [12, 32]. At its core, TSF is concerned with constructing predictive models for time-dependent sequential data. This involves leveraging historical patterns and relationships within observations to forecast future data points. The methodologies employed in TSF are diverse, ranging from classical statistical approaches, such as Autoregressive Integrated Moving Average (ARIMA) [18] and Exponential Smoothing (ETS) [5], to deep learning (DL) approaches, including Multi-Layer Perceptrons (MLPs) [42], Recurrent Neural Networks (RNNs) [43], Long Short-Term Memory (LSTMs) [35], Temporal Convolutional Networks (TCNs) [16], and Transformer architectures [27, 21]. More recently, the field has witnessed the appearance of foundation Large Time-Series Models (LTSMs), pre-trained on extensive time-series datasets to enable zero-shot forecasting. These models, including Timer [24], Moirai [38], TimesFM [10], Chronos [1], Moment [13], and Toto [9] predominantly utilize variations of the Transformer architecture.

Generally, TSF methodologies prioritize the minimization of predictive error, often neglecting the integration of predicted outputs within subsequent downstream processes. In numerous downstream applications of forecasting, the practical significance of forecast errors is not uniform, and this treatment introduces suboptimal model performance with respect to the ultimately desired objective. This is effectively illustrated by forecasting challenges *IEEE-CIS Technical Challenge on Predict+Optimize for Renewable Energy Scheduling* [3] and the *M5 Accuracy Competition* [3], where evaluations based solely on forecast accuracy substantially mismatches with evaluations based on the eventual optimization objective, such as energy minimization. This necessitates the development of TSF models that explicitly incorporate downstream task objectives during development and evaluation. This integration is essential given the widespread of real world analytical systems combining predictive and optimization components. For example, Bertsimas and Kallus [4] propose learning weight functions from data for integration into optimization objectives. Similarly, Elmachtoub and Grigas [11] proposed a “Predict-then-Optimize” framework within linear programming, directly leveraging optimization structure to inform loss function design. Furthermore, the ML community has witnessed a significant trend towards end-to-end (E2E) learning paradigms, applied across domains such as finance [2], image recognition [36], robotic manipulation [19], and inventory-management [30] highlighting the potential for this approach in TSF.

A major limitation within existing literature [4, 11, 30] is the assumption of pre-defined task specifications. Specifically, these methodologies presuppose that regions of forecasting importance are both provided and static. However, numerous real-world TSF applications, such as wireless traffic prediction, necessitate adaptive approaches due to unknown and dynamically shifting importance regions. For instance, in energy efficiency policies, low-traffic periods are more important for base-station deactivation, while high-traffic periods are less relevant. Conversely, power allocation strategies may require sensitivity to both extremes, with lower importance on intermediate values. In practice, these thresholds are often not known a priori and potentially time-varying. Consequently, there is a pressing need for TSF frameworks that enable post-hoc configuration to give importance to specific regions of interest during inference. This work takes the first step, to the best of our knowledge, to address the observed gap. A motivating problem that can be tackled by our approach is illustrated in Figure 1.

Contributions. The specific contributions of this work are outlined as follows: (i) This research introduces a new training methodology that modifies current multivariate TSF models enabling adaptation to multiple downstream tasks at inference-time. A comprehensive empirical evaluation, including thorough baseline comparisons and ablation studies showcase the efficacy of the proposed scheme. (ii) The performance of the proposed models was assessed using a synthetic trace and well as several real-world traces. In addition, we intend release a new wireless mobile network dataset.

Outline of Paper. This paper proceeds as follows. Section 2 reviews the related literature. Section 3 formalizes the forecasting problem. Section 4 details the methodology employed in this research. Section 5 describes the experiments we performed to investigate the performance of our training methodology. Finally, Section 6 concludes the paper and outlines avenues for future research.

2 Literature Review

Time-Series Forecasting. Traditionally, statistical approaches like ARIMA [18] and ETS [5] were predominant in TSF. However, the surge in computational power and data availability has spurred the adoption of deep learning techniques. This transition encompasses MLPs [42], RNNs [43], LSTMs [35], TCNs [16], and Transformer architectures [27, 21, 39, 45, 46]. Adapting Transformers for TSF is now a key research area, with efforts focused on: (1) refining internal components, particularly attention mechanisms [39, 45, 46]; (2) transforming input token representations using techniques like stationarization [23], channel independence [27], and patching [27, 21]; and (3) broadly modifying the

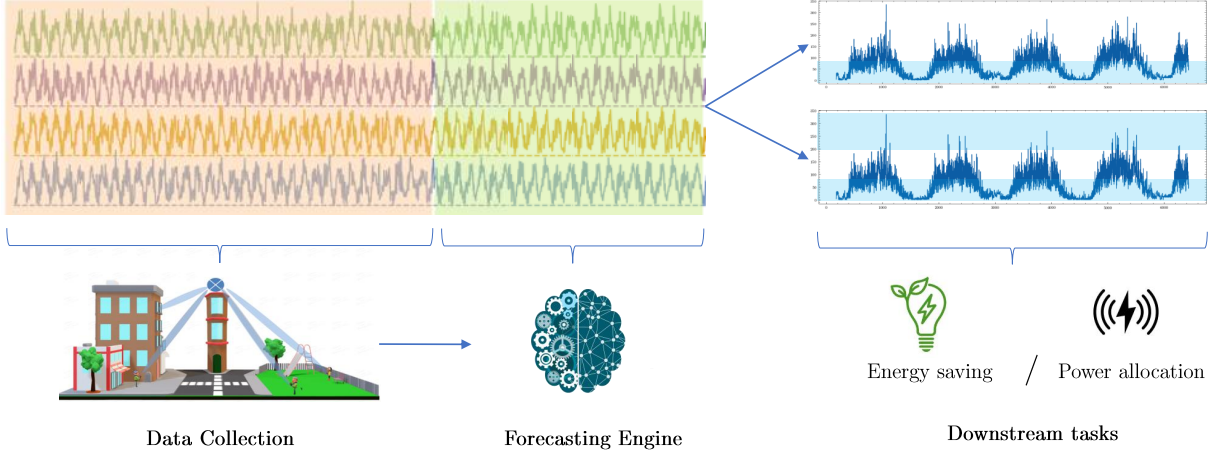


Figure 1: This figure illustrates the time-series forecasting problem in a wireless network context. The process involves data collection to gather historical time-series information, followed by the development and training of a forecasting model to predict future values. These forecasts are then used for downstream applications. In this example, we show two downstream tasks: energy efficiency policy and power allocation. For energy efficiency, accurate forecasts during low-traffic periods are crucial, as indicated by the highlighted blue interval, to optimize base-station deactivation high-traffic periods are less critical. Power allocation, however, requires accurate forecasts across both high and low traffic periods, also highlighted in blue, with less emphasis on intermediate values. Traditional forecasting methods treat prediction as an independent problem, neglecting the specific requirements of downstream tasks. This is suboptimal because different applications have varying sensitivities to different forecast ranges. A second approach considers an E2E system tailored to a specific downstream task. This work advances this concept by enabling the forecasting model to adapt to different downstream tasks during inference.

Transformer architecture and its modules [44]. Recent advances include foundation LSTMs like Timer [24], Moirai [38], TimesFM [10], Chronos [1], Moment [13], and Toto [9] which leverage pre-training and Transformer variants for zero-shot forecasting. This research extends state-of-the-art transformer architectures by integrating a task-specific configuration mechanism, enabling dynamic adaptation of model predictions during inference.

Task-Aware Forecasting. Prior research has explored customizations of the objective function for TSF, through loss reshaping or re-weighting [29, 41, 8, 17]. These works primarily aim to integrate uncertainty quantification or fairness considerations, diverging from the objective of tailoring models to specific downstream tasks. Conversely, other research have concentrated on developing frameworks that derive loss weights from downstream task characteristics, thereby guiding the training process of forecasting models [3, 11, 14]. While our methodology shares conceptual similarities with this latter line of work, specifically in the incorporation of loss shaping during training, it distinguishes itself by proposing a training methodology that enables the same model to accommodate diverse downstream task requirements at inference-time.

3 The Forecasting Problem

Time-Series. A multivariate time-series is a sequence of vector-valued observations ordered temporally. Let $\mathbf{x}_t \in \mathbb{R}^n$ denote a n -dimensional real-valued vector observed at time t , where $t \in [T]$ and $n \geq 1$. The full time-series is represented as the ordered set $\{\mathbf{x}_1, \mathbf{x}_2, \dots, \mathbf{x}_T\}$, where each $\mathbf{x}_t = (x_{t,i})_{i \in [n]}$ corresponds to measurements of n variables at time t . The temporal dependency between observations is intrinsic to the series, with \mathbf{x}_t potentially influenced by past values \mathbf{x}_{t-k} for some lag $k > 0$. We assume each series $i \in [n]$ lies within a bounded set $\mathcal{X} \subset \mathbb{R}$, where $|\mathcal{X}| < \infty$.

The Learning Problem. Time-series forecasting is reformulated as a supervised regression task by constructing input-output pairs from sliding windows over the series. Let $\tau \in \mathbb{N}$ be the forecast horizon and $w \in \mathbb{N}$ be the window size. In practice, the window size w is treated as a hyperparameter. For each time t , the input $\mathbf{X}_t = \mathbf{x}_{t-w:t-1} \in \mathcal{X}^{w \times n}$ consists of a history window $\{\mathbf{x}_{t-w}, \dots, \mathbf{x}_{t-1}\}$, and the target $\mathbf{Y}_t = \mathbf{x}_{t:t+\tau-1} \in \mathcal{X}^{\tau \times n}$ is the future window $\{\mathbf{x}_t, \dots, \mathbf{x}_{t+\tau-1}\}$. The mapping $f_\theta : \mathcal{X}^{w \times n} \rightarrow \mathcal{X}^{\tau \times n}$, parameterized by θ , is learned to approximate the underlying dynamic $\mathbf{Y}_t = f(\mathbf{X}_t) + \epsilon_t$, where $\epsilon_t \in \mathbb{R}^{\tau \times n}$ is noise and f is some unknown dynamic. This generates a dataset

$D = \{(\mathbf{X}_t, \mathbf{Y}_t)\}_{t=w}^{T-\tau}$. The goal is to learn the model $\theta_* \in \mathbb{R}^d$ for $d \geq 1$ that minimizes the expected loss over the data distribution $\mathcal{D}(\mathbf{X}, \mathbf{Y})$:

$$\theta_* \in \arg \min_{\theta \in \mathbb{R}^d} \mathbb{E}_{(\mathbf{X}, \mathbf{Y}) \sim \mathcal{D}} [l(f_\theta(\mathbf{X}), \mathbf{Y})], \quad (1)$$

where $l : \mathbb{R}^{\tau \times n} \times \mathbb{R}^{\tau \times n} \rightarrow \mathbb{R}$ is a differentiable loss function. In practice, this expectation is approximated by the empirical risk over D : $\tilde{\theta}_* \in \arg \min_{\theta} \frac{1}{|D|} \sum_{(\mathbf{X}_t, \mathbf{Y}_t) \in D} l(f_\theta(\mathbf{X}_t), \mathbf{Y}_t) + R(\theta)$. The regularization term $R : \mathbb{R}^d \rightarrow \mathbb{R}$ (e.g., the Euclidean distance $R(\theta) = \lambda \|\theta\|_2^2$) is incorporated to control the complexity of the model parameters θ , and it aims to prevent the memorization of noise within the training data, enhancing the model’s ability to generalize to novel data [34]. Among the most commonly used loss functions are the Mean Squared Error (MSE) and the Mean Absolute Error (MAE), each of which serves a distinct statistical purpose (i.e., conditional expectation and the conditional median, respectively).

4 Methodology

Our methodological investigation proceeds by first establishing a baseline policy (B-POLICY), representative of standard forecasting model training that overlooks specific prediction intervals. We then define an end-to-end policy (E2E-POLICY), which focuses on training a model tailored to a particular interval of interest. Subsequently, we introduce a naive policy (C-POLICY) designed to train a foundation model capable of adapting to various intervals at inference time by exposing it to all possible intervals during training. Following this, we describe a policy (D_L-POLICY) that explores a finite subset of relevant intervals, strategically chosen such that their combination covers the entire forecasting space. Finally, we propose a policy (D_L*-POLICY) that discretizes the forecasting space and, when integrated with a patching technique, can enable the training of more effective foundation models.

Baseline Policy (B-POLICY). This policy follows the baseline training procedure detailed in Section 3. This training approach does not incorporate interval sensitivity, and the loss is computed with respect to the forecasting target over the domain \mathcal{X} .

Task-specific Policy (E2E-POLICY). Given a target interval $\mathcal{I} \subseteq \mathcal{X}$, the task-specific policy only considers a forecasting target within this range. In particular, this policy can be considered as a variation of the baseline policy limited to consider a forecasting loss solely over the intervals of interest. Our goal is to learn the model $\theta_* \in \mathbb{R}^d$ that minimizes the interval-specific expected loss over a data distribution $\mathcal{D}(\mathbf{X}, \mathbf{Y})$ given as $\tilde{\theta}_* \in \arg \min_{\theta \in \mathbb{R}^d} \mathbb{E}_{(\mathbf{X}, \mathbf{Y}) \sim \mathcal{D}} [l(f_\theta(\mathbf{X}), \mathbf{Y}) \cdot \mathbb{1}(\mathbf{Y} \in \mathcal{I}^{\tau \times n})]$, where $\mathbb{1}(\chi) \in \{0, 1\}$ is the indicator function equal to 1 when condition χ is true. Again, the expectation can be approximated by the interval-specific empirical risk over some dataset D consisting of samples from \mathcal{D} with a regularization term.

Continuous-Interval Training Policy (C-POLICY). To allow the forecasting model to differentiate between any target intervals within \mathcal{X} , we incorporate the interval as a covariate. A covariate interval $\mathcal{I} \subseteq \mathcal{X}$ is represented as a two-dimensional vector in \mathcal{X}^2 containing its boundary values (e.g., a vector encoding $(I_{\min}, I_{\max}) \in \mathcal{X}^2$, for some interval $[I_{\min}, I_{\max}] \subseteq \mathcal{X}$). This enables the model to learn the relationship between varying intervals and its predictive outputs. Specifically, the learned mapping f_θ becomes a function of both the input time-series \mathbf{X} and the interval \mathcal{I} , i.e., the mapping $f_\theta : \mathcal{X}^{w \times n+2} \rightarrow \mathcal{X}^{\tau \times n}$. During training, we sample intervals uniformly at random over the set $\mathcal{U}_\delta = \{\mathcal{I} \subset \mathcal{X} : |\mathcal{I}| \geq \delta\}$, where δ represents the minimum length of the sampled intervals. The minimal distance constraint is introduced to make the training more stable, because small intervals contain less samples introducing high variance. This is further demonstrated numerically in Figure 4f. Consequently, for a data sample $(\mathbf{X}_t, \mathbf{Y}_t) \sim \mathcal{D}$ and its corresponding sampled interval \mathcal{I}_t , our custom loss function is defined as:

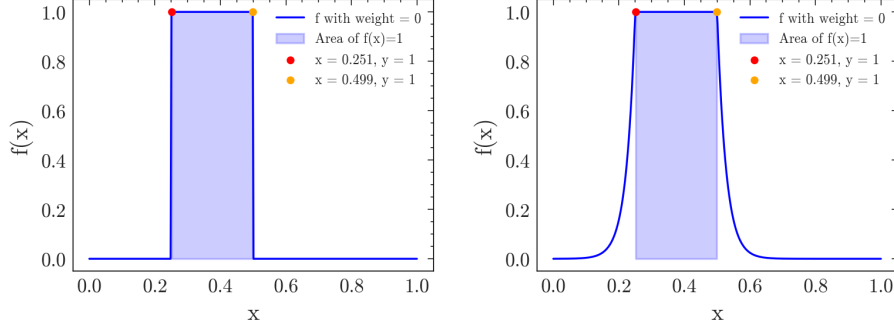
$$L(f_\theta(\mathbf{X}_t, \mathcal{I}_t), \mathbf{Y}_t, \mathcal{I}_t) = l(f_\theta(\mathbf{X}_t, \mathcal{I}_t), \mathbf{Y}_t) \cdot \mathbb{1}(\mathbf{Y}_t \in \mathcal{I}_t^{\tau \times n}). \quad (2)$$

Thus, our training objective is to learn the model parameters $\theta_{\text{Cont}}^* \in \mathbb{R}^d$ ($d \geq 1$) that minimize the interval-uniform expected loss over the data distribution $\mathcal{D}(\mathbf{X}, \mathbf{Y})$ and the interval distribution \mathcal{U}_δ :

$$\theta_* \in \arg \min_{\theta \in \mathbb{R}^d} \mathbb{E}_{(\mathbf{X}, \mathbf{Y}) \sim \mathcal{D}, \mathcal{I} \sim \mathcal{U}_\delta} [L(f_\theta(\mathbf{X}, \mathcal{I}), \mathbf{Y}, \mathcal{I})]. \quad (3)$$

Similar to the previous policies, the above problem is approximated by minimizing the empirical risk over the dataset D and the interval distribution \mathcal{U}_δ : $\tilde{\theta}_* \in \arg \min_{\theta \in \mathbb{R}^d} \frac{1}{|D|} \sum_{(\mathbf{X}_t, \mathbf{Y}_t) \in D} L(f_\theta(\mathbf{X}_t, \mathcal{I}_t), \mathbf{Y}_t, \mathcal{I}_t) + R(\theta)$, where \mathcal{I}_t is the sampled interval from \mathcal{U}_δ for each $(\mathbf{X}_t, \mathbf{Y}_t) \in D$.

Discretized-Interval Training Policy (D_L-POLICY). This policy closely resembles the C-POLICY, except that the support space of the distribution of possible interval is severely reduced. In particular, the interval selection process now involves sampling an interval from a discrete distribution, denoted by \mathcal{C}_L , defined over a set of L disjoint intervals that collectively cover the interval \mathcal{X} , i.e., for a given L the support $\text{supp}(\mathcal{C}_L)$ satisfies $\bigcup_{\mathcal{I} \in \text{supp}(\mathcal{C}_L)} \mathcal{I} = \mathcal{X}$ where \bigcup denotes the union of disjoint sets.



(a) The weighing mechanism for values inside interval $[0.25, 0.5]$ with a large decay rate $\nu \rightarrow \infty$. (b) The weighing mechanism for values inside interval $[0.25, 0.5]$ with decay rate $\nu = 37$.

Figure 2: This figure depicts the decay function with varying decay rates, illustrating how different rates influence the smoothness of the transition in importance for values outside the interval of interest.

Patching-Augmented Discretized Training Policy (D_L^* -Policy). The premise behind the design of this policy is to consider the D_L -Policy configured with a sufficiently large L corresponding to a finer discretization of the domain \mathcal{X} . At inference time when requested with an unknown interval \mathcal{I} , the policy combines the constituent intervals to make the predictions. This is made possible with two main modifications. First, the loss function incorporates a decay function that modulates the contribution of each sample to the loss based on its distance from the center of its associated interval.⁴ This decay mechanism is defined as

$$d_\nu(y, \mathcal{I}) = \exp(-\nu \cdot \max(0, |y - \Delta_{\text{avg}}| - \Delta_{\text{diff}})), \quad (4)$$

where ν is the decay rate, and $\Delta_{\text{avg}} = \frac{\max(\mathcal{I}) + \min(\mathcal{I})}{2}$ is the midpoint of an interval and $\Delta_{\text{diff}} = \frac{\max(\mathcal{I}) - \min(\mathcal{I})}{2}$ is half of the length of the interval.

As the decay rate ν becomes large ($\nu \rightarrow \infty$), the weight $\prod_{i \in [n], t \in [\tau]} d_\nu(y_i, \mathcal{I}) \in [0, 1]$ converges to the indicator function $\mathbb{1}(\mathbf{Y} \in \mathcal{I}^{n \times \tau}) \in \{0, 1\}$ in Eq. (2). This weighting allows learning at interval boundaries and introduces a soft overlap between intervals, which is beneficial for reducing patching errors caused by boundary uncertainties. Additionally, a classification head $f_\theta^c: \mathcal{X}^{w \times n+2} \rightarrow [0, 1]^{\tau \times n}$ (parameterized by a shared θ) is appended to predict if the true value falls within \mathcal{I}_t , using the same notation as before. The modified regression loss with the soft boundary is $L_\nu(f_\theta(\mathbf{X}_t, \mathcal{I}_t), \mathbf{Y}_t, \mathcal{I}_t) \triangleq l(f_\theta(\mathbf{X}_t, \mathcal{I}_t), \mathbf{Y}_t) \cdot \prod_{i \in [n], t \in [\tau]} d_\nu(y_{t,i}, \mathcal{I}_t)$, and the modified classification loss is $L'_\nu(f_\theta^c(\mathbf{X}_t, \mathcal{I}_t), \mathbb{1}(\mathbf{Y}_t \in \mathcal{I}_t), \mathcal{I}_t) \triangleq l'_\nu(f_\theta^c(\mathbf{X}_t, \mathcal{I}_t), \mathbb{1}(\mathbf{Y}_t \in \mathcal{I}_t)) \cdot \prod_{i \in [n], t \in [\tau]} d_\nu(y_{t,i}, \mathcal{I}_t)$, where l'_ν is a classification loss like cross entropy. The learning objective for the augmented model parameters (including the classifier) is defined as follows:

$$\theta_\star \in \arg \min_{\theta \in \mathbb{R}^d} \mathbb{E}_{(\mathbf{X}, \mathbf{Y}) \sim \mathcal{D}, \mathcal{I} \sim \mathcal{C}_L} [L_\nu(f_\theta(\mathbf{X}, \mathcal{I}), \mathbf{Y}, \mathcal{I}) + \phi \cdot L'_\nu(f_\theta^c(\mathbf{X}, \mathcal{I}), \mathbb{1}(\mathbf{Y} \in \mathcal{I}), \mathcal{I})], \quad (5)$$

where $\phi \in [0, 1]$ is a hyperparameter introduced to balance the importance of the regression and classification tasks. This objective is approximated empirically using the dataset D and the interval distribution \mathcal{C}_L :

$$\tilde{\theta}_\star \in \arg \min_{\theta \in \mathbb{R}^d} \frac{1}{|D|} \sum_{(\mathbf{X}_t, \mathbf{Y}_t) \in D} (L_\nu(f_\theta(\mathbf{X}_t, \mathcal{I}_t), \mathbf{Y}_t, \mathcal{I}_t) + \phi \cdot L'_\nu(f_\theta^c(\mathbf{X}_t, \mathcal{I}_t), \mathbb{1}(\mathbf{Y}_t \in \mathcal{I}_t), \mathcal{I}_t)) + R(\theta),$$

where \mathcal{I}_t is the sampled interval from \mathcal{C}_t for each $(\mathbf{X}_t, \mathbf{Y}_t) \in D$.

Patching Mechanism. Given an arbitrary interval \mathcal{I} , we first identify the subset of training intervals that intersect with \mathcal{I} , given by the mapping

$$\Xi_L(\mathcal{I}) \triangleq \{\mathcal{I}' \in \text{supp}(\mathcal{C}_L) : \mathcal{I}' \cap \mathcal{I} \neq \emptyset\}, \quad (6)$$

where $\text{supp}(\mathcal{C}_L)$ is the support of the distribution \mathcal{C}_L of size L . The logic behind this is that when L is large enough, the union of intervals in $\Xi_L(\mathcal{I})$ is a good approximation of \mathcal{I} . For an input series \mathbf{X} and target interval \mathcal{I} the patching mechanism strategies are defined as follows:

⁴This function is depicted in Figure 2.

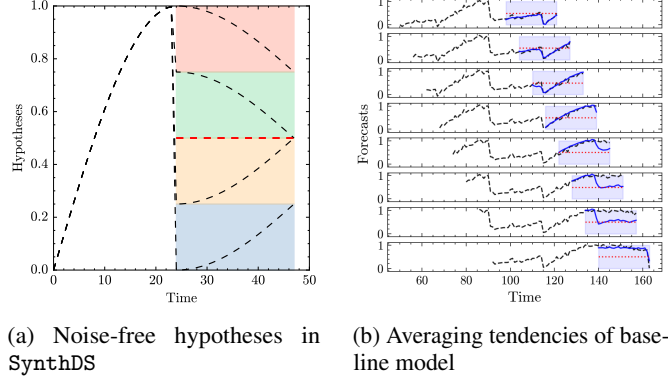


Figure 3: Subfigure (a) depicts the expected hypotheses used to construct the synthetic trace SynthDS. Subfigure (b) depicts the inability of the baseline policy B-POLICY to distinguish between the different patterns in SynthDS dataset, as it predicts the average hypothesis (red line at 0.5). The model used is a trained iTransformer. Each subplot shows a time-shift of six steps. The black dotted line indicates the true values. The blue line shows the model’s predictions. The shaded region depicts the forecasting horizon.

- *Averaging Strategy (1-strategy)*. This strategy computes a weighted average of the regression predictions for all intersecting training intervals, weighted by their respective classification probabilities for the given input and the target interval \mathcal{I} . Formally, defined as

$$\hat{\mathbf{Y}} = \frac{\sum_{\mathcal{I}' \in \Xi_L(\mathcal{I})} f_{\theta}^c(\mathbf{X}, \mathcal{I}') f_{\theta}(\mathbf{X}, \mathcal{I}')}{\sum_{\mathcal{I}' \in \Xi_L(\mathcal{I})} f_{\theta}^c(\mathbf{X}, \mathcal{I}')}. \quad (7)$$

- *Maximum Confidence Strategy (∞ -strategy)*. This strategy selects the regression prediction corresponding to the training interval with the highest classification probability for the given input and the target interval \mathcal{I} . Formally, defined as

$$\hat{\mathbf{Y}} = f_{\theta}(\mathbf{X}, \operatorname{argmax}_{\mathcal{I}' \in \Xi_L(\mathcal{I})} f_{\theta}^c(\mathbf{X}, \mathcal{I}')). \quad (8)$$

5 Experiments

This section presents the numerical results of our training methodology and compares its forecasting performance with several baselines. We start by outlining the forecasting models, training policies, benchmark datasets, and training configurations used. Following this, we provide a quantitative analysis of the different training strategies applied to these models.⁵

5.1 Experimental Setup

Time-Series Forecasting Models. We evaluate four leading time series forecasting models: iTransformer [22], DLinear [42], PatchTST [28], and TimeMixer [37]. To incorporate target interval information \mathcal{I} , we modified these architectures. Given an interval of interest $\mathcal{I} \subseteq \mathcal{X}$, for iTransformer, the vectorized form of \mathcal{I} was concatenated to the temporal encoding. For DLinear, PatchTST, and TimeMixer, \mathcal{I} ’s vectorized encoding was added as two extra temporal channels. Furthermore, we adapted these regression models for a dual-task objective (regression and classification) by adding a classification head. This involved doubling the final projection layer’s output size (τ , the forecasting horizon) and splitting it into regression forecasts (first τ dimensions) and classification logits (remaining τ dimensions). This modification allows the models to predict future values and simultaneously assess the probability of these forecasts falling within the target interval \mathcal{I} .

Training Policies. We evaluate the training policies introduced in Section 4, namely B-POLICY, E2E-POLICY, C-POLICY, D_L -POLICY, and D_L^* -POLICY. The \star in the latter denotes either average (1) or maximum (∞) patching.

Benchmarking Datasets. In our experimental evaluation, we employ several benchmark datasets to substantiate our claims: (i) SynthDS is a synthetic dataset used to highlight the various components of our proposed methodology. We

⁵The code is publicly available github.com/netop-team/gotsf.

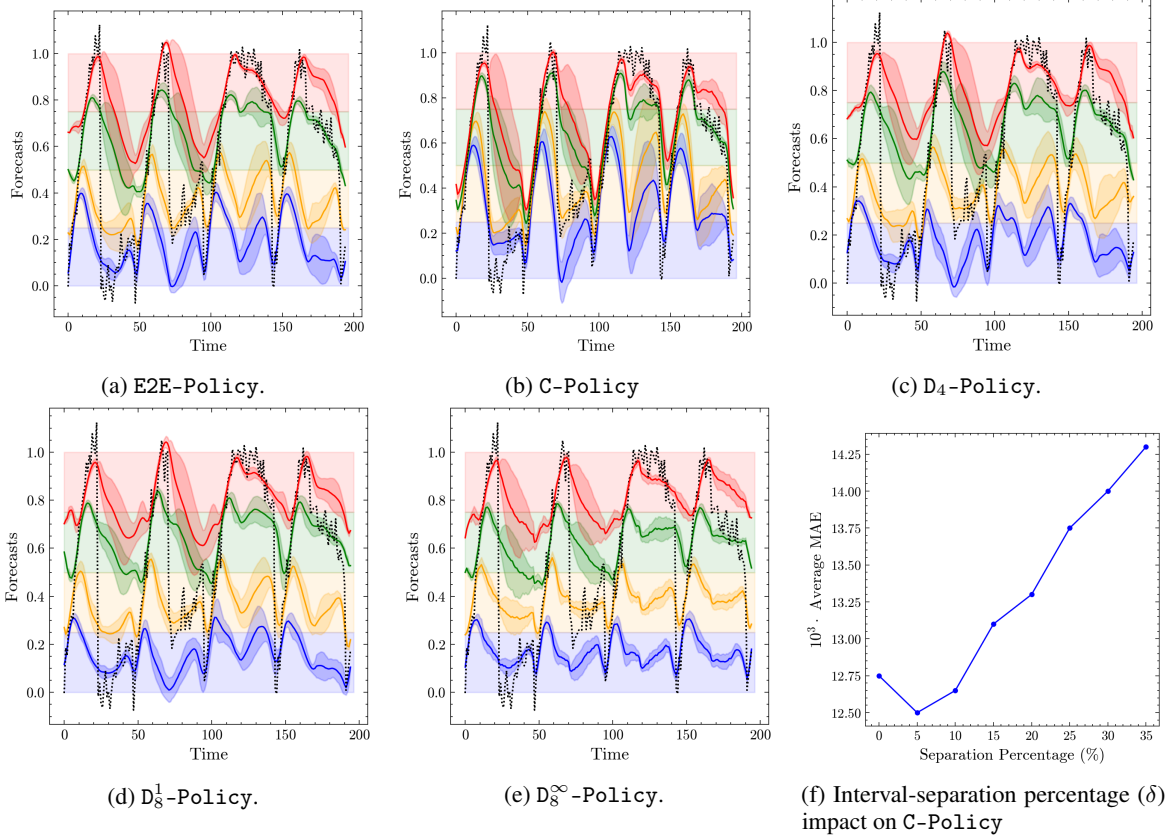


Figure 4: Subfigures (a) and (b) illustrate the performance of the iTransformer model trained with the E2E-Policy and C-Policy, respectively. Subfigure (c) investigates the impact of the additional hyperparameter (δ) within the C-Policy. Target forecast values are indicated by black dotted lines, while solid lines represent the mean prediction at each time step, with the shaded area denoting the standard deviation. Colored regions (red, green, yellow, and blue) delineate the different intervals of interest. Subfigures (c)–(e) provide a qualitative comparison of the D_4 -Policy, D_8^∞ -Policy, and D_8^1 -Policy training schemes applied to the iTransformer model on the SynthDS dataset, where patching involved combining eight intervals into four.

construct the trace by combining an input signal $\mathbf{s} = \left(\sin\left(\frac{\pi n}{2D}\right)\right)_{n \in [w]}$, where $w = 24$ represents the length of the signal, and a corresponding output signal selected uniformly at random (u.a.r.) from the set $\left\{0.25 \left(\sin\left(\frac{\pi}{2w}n + \frac{\pi}{2}\right) + k\right)\right\}_{n \in [w]} : k \in [4]$. To generate a trace spanning $T = 3.1 \times 10^3$ timesteps, we concatenate the same randomly selected signal multiple times. Subsequently, we introduce Gaussian noise to the trace, where the noise has a mean of 0 and a standard deviation of 0.05. A noise-free version of this trace is depicted in Figure 3a. (ii) BLW-TrafficDS is released to the public domain as part of this study.⁶ The dataset comprises a wireless beam-level traffic volume containing 100 beams and 10^3 timesteps. (iii) Traffic [6] contains hourly road occupancy rates (ranging from 0 to 1) recorded by sensors on San Francisco Bay area freeways from 2015 to 2016, totaling 48 months of data. (iv) Electricity [33] includes hourly electricity consumption (in kWh) records of 321 clients from 2012 to 2014. (v) Weather [39] contains 21 meteorological indicators, such as air temperature and humidity, recorded every 10 minutes throughout the entire year of 2020.

Training Configuration. To ensure the reproducibility of our experiments, we provide a comprehensive description of the training setup. The datasets were divided into training, validation, and testing subsets. A 66-17-17 split was used for the SynthDS, Traffic, Electricity, and Weather datasets, while the BLW-TrafficDS dataset used a 70-10-20 split. Four state-of-the-art time series forecasting models—iTransformer, DLinear, PatchTST, and TimeMixer—were evaluated across the designated tasks.

The BLW-TrafficDS, Traffic, Electricity, and Weather datasets were processed using a multivariate-to-multivariate configuration, whereas the SynthDS dataset used a univariate-to-univariate setup. Input sequence lengths

⁶The dataset is publicly released huggingface.co/datasets/netop/Beam-Level-Traffic-Timeseries-Dataset.

and forecasting horizons were tailored to each dataset: 48/24 for SynthDS, 96/24 for BLW-TrafficDS, and 168/48 for Traffic, Electricity, and Weather. The number of input channels was cropped to 100 for all datasets except Weather, which used 21 channels due to its limited dimensionality.

Model configurations across all experiments included 3 layers with a model dimension of 256. TimeMixer was configured with a channel dimension of 100. All models were trained with a batch size of 32 for 50 epochs. The AdamW optimizer [25] was used with an initial learning rate of 10^{-3} and a cosine annealing schedule with $\eta_{\min} = 10^{-5}$, defined as: $\eta_t = \eta_{\min} + 0.5(\eta_{\max} - \eta_{\min})(1 + \cos(\pi \cdot t/n_{\text{epochs}}))$.

The MAE loss was used for regression tasks, while Binary Cross Entropy loss was applied for classification tasks when applicable. Early stopping with a patience of 5 epochs and checkpoint saving mechanisms were employed to reduce overfitting. Validation loss was computed as the average loss over each training interval.

The D_L^* -Policy was evaluated using 4 and 8 intervals for the SynthDS, Traffic, Electricity, and Weather datasets, and 8 and 16 intervals for the BLW-TrafficDS dataset. Interval endpoint sampling was performed per sample within each batch and incorporated into the forward pass as detailed in Section 4.

The dataset sizes are as follows: Weather—52,696 points, Traffic—17,544 points, and Electricity—26,304 points. To set forecasting boundaries, the maximum values were assigned as $\max(\mathcal{X}) \in \{0.2, 500.0, 10000.0\}$ for Traffic, Weather, and Electricity, respectively. All experiments were executed on a system with 6 Tesla V100/16GB GPUs and an Intel(R) Xeon(R) Platinum 8164 CPU (104 cores).

5.2 Numerical Results

Qualitative Comparison of Training Schemes. To gain intuitive understanding of how different training policies behave when downstream tasks specify an interval of interest (leading training to prioritize accuracy within that interval), we focus our initial evaluation on training the iTransformer model on the SynthDS trace due to its simplicity for interpreting results and qualitatively assessing performance.

Baseline. We first analyze the baseline policy’s averaging behavior when training iTransformer on SynthDS. As shown in Figure 3b, the model learns an averaged prediction, converging to the trace’s midpoint ($1/2$), indicating its insensitivity to specific intervals of interest.

End-to-End Training Approach. Figure 4a examines E2E-Policy with the iTransformer model, targeting one of four specific intervals: $\{\mathcal{I}_i : i \in [4]\} \triangleq \{[0, 0.25], [0.25, 0.5], [0.5, 0.75], [0.75, 1]\}$. This represents an end-to-end strategy where the forecasting loss is adapted to emphasize task-relevant intervals. These intervals embody distinct hypotheses, and this policy serves as an optimal benchmark, illustrating the best-case performance achievable by a policy adaptable to any interval and configurable at inference.

Continuous Exploration of Intervals. We also evaluate C-Policy using the iTransformer model on SynthDS. The results in Figure 4b indicate that this approach struggles to effectively learn the relationship between intervals of interest and their corresponding hypotheses, highlighting the difficulty of the learning task even in a synthetic setting. The model is tasked with learning a mapping from every possible interval $\mathcal{I} \subset \mathcal{X}$ to its associated hypothesis. Further, Figure 4f explores the impact of restricting the support space of training intervals by enforcing a minimum separation $|\mathcal{I}| \geq \delta$. While performance improves with a reduced sampling space, beyond a certain threshold δ' , it deteriorates due to the model overshooting the true interval lengths and introducing bias.

Targeted Exploration of Intervals. Building on the observed limitations of continuous exploration, Figure 4c investigates a discrete policy (D_L -Policy) on SynthDS. This policy uniformly samples from a predefined, finite, and smaller set of intervals of interest at training time. We first test this with the optimal E2E-Policy, which can perfectly distinguish signal patterns. The results demonstrate that D_L -Policy achieves comparable performance to E2E-Policy while offering the advantage of inference-time adaptability to various downstream tasks. However, this approach assumes prior knowledge of the relevant interval set (or its size), which motivates the subsequent experiment where we intentionally increase the number of considered intervals to demonstrate the reconstructability of the true signal.

Adaptive Interval Exploration with Patching Techniques. Figures 4d and 4e investigate the effectiveness of our patching strategies—averaging and the maximum confidence approach (detailed in Section 4)—in capturing underlying dynamics on SynthDS when the number of considered intervals intentionally exceeds the true quantity. This deliberate increase aims to qualitatively assess the robustness of the patching schemes. While the patching schemes exhibit visually similar performance, a quantitative analysis will provide further elaboration. Notably, these schemes more clearly distinguish the four distinct underlying hypotheses used to construct the synthetic trace compared to the C-Policy, thus effectively motivating the design of our approach. This design involves training a model on a large set of intervals that can be combined at inference time to generate focused forecasts for a specific interval of interest.

Quantitative Comparison of Training Schemes. Following our qualitative evaluation of the proposed training policies, Table 1 and Table 2 present the numerical results we obtained on the SynthDS and BLW-TrafficDS datasets, respectively. These tables display the MAE values for the four models, each trained with the four distinct policies.

Table 1 shows the result of training the different models on the SynthDS trace. We observe comparable performance between the iTransformer and PatchTST policies. Notably, the B-Policy, which does not incorporate inference-

Mod.	Train Strat.	\mathcal{I}_1	\mathcal{I}_2	\mathcal{I}_3	\mathcal{I}_4	Avg.	Mod.	Train Strat.	\mathcal{I}_1	\mathcal{I}_2	\mathcal{I}_3	\mathcal{I}_4	Avg.
DLinear	D ₄ -Policy	15.036	11.678	11.735	16.825	13.818	TimeMixer	D ₄ -Policy	16.207	11.420	11.489	15.503	13.655
	D ₈ ¹ -Policy	14.538	11.949	11.247	16.782	13.629		D ₈ ¹ -Policy	15.719	12.236	11.747	17.294	14.249
	D ₈ [∞] -Policy	18.513	12.782	10.723	18.212	15.057		D ₈ [∞] -Policy	17.895	15.048	13.291	19.693	16.482
	B-Policy	50.942	20.285	17.074	40.994	32.324		B-Policy	45.535	18.831	13.902	34.852	28.280
	C _{0.1} -Policy	24.805	12.846	10.574	20.340	17.141		C _{0.1} -Policy	17.515	13.515	10.783	16.570	14.596
	Improvement	71.46%	42.43%	38.07%	59.06%	57.89%		Improvement	65.48%	39.35%	22.44%	55.52%	51.72%
PatchTST	D ₄ -Policy	13.183	9.083	7.736	12.697	10.675	iTransformer	D ₄ -Policy	14.142	7.960	7.968	13.116	10.796
	D ₈ ¹ -Policy	13.210	10.180	8.606	12.851	11.212		D ₈ ¹ -Policy	14.096	9.168	8.377	12.427	11.017
	D ₈ [∞] -Policy	15.146	11.240	8.919	13.290	12.149		D ₈ [∞] -Policy	17.493	9.646	8.631	13.598	12.342
	B-Policy	37.883	26.799	14.877	36.842	29.100		B-Policy	40.213	26.184	16.239	33.737	29.093
	C _{0.1} -Policy	15.343	10.967	9.186	13.669	12.291		C _{0.1} -Policy	19.999	10.587	8.707	13.378	13.168
	Improvement	65.20%	66.18%	48.00%	65.55%	63.32%		Improvement	64.95%	69.60%	50.94%	63.17%	62.89%

Table 1: MAE values ($\times 10^3$) for the four different models (DLinear, TimeMixer, iTransformer, and PatchTST) trained with the four policies (D₄-Policy, D₈¹-Policy, D₈[∞]-Policy, B-Policy, and C_{0.1}-Policy) on the SynthDS trace. The highlighted values represent the lowest MAEs for a specific model in its respective column, while the underlined values represent the overall lowest MAEs for their respective columns. The improvement of a model is measured as a comparison between the best performing training policy and the baseline policy. The intervals of interest, denoted as \mathcal{I}_1 , \mathcal{I}_2 , \mathcal{I}_3 , and \mathcal{I}_4 , correspond to a partition of the time series range \mathcal{X} into four contiguous sub-intervals of equal length.

time adaptation of the interval of interest, exhibits the poorest performance. The C-Policy demonstrates a modest improvement in MAE, indicating that training towards specific intervals offers some benefit. However, sampling all possible intervals in the C-Policy hinders the model’s ability to learn distinct underlying hypotheses, as evidenced by the superior performance of the D_L-Policy, which we configure with four specific intervals. Introducing the patching mechanism in D_L^{*}-Policy leads to some performance degradation across certain intervals. Nevertheless, its overall MAE remains comparable to, and occasionally slightly surpasses, that of the D_L-Policy, potentially due to an ensemble-like noise reduction effect. Table 2 displays the results of training the different models on the BLW-TrafficDS trace. We observe that the same conclusions generally extend to this real-world trace. However, we note that patching actually outperforms the vanilla discrete approach, with patching using the averaging strategy yielding the best performance under the PatchTST model. We observe that the conclusions change for weaker models such as DLinear, where the C-Policy appears to dominate. However, given its exceedingly lower overall performance compared to the other models, the order of improvement can be influenced by random factors. We recall that we optimally configure the D_L-Policy with intervals precisely delineating the distinct underlying hypotheses, a priori knowledge unlikely to be available in practical scenarios. Consequently, the D_L^{*}-Policy presents a pragmatic approach and a viable solution for training foundational models capable of adapting to varying intervals during inference.⁷

6 Conclusion

This research introduces a novel training methodology designed to transform existing TSF models into foundational architectures capable of inference-time adaptation for diverse downstream tasks. A comprehensive empirical evaluation was performed to ascertain the efficacy of the proposed approach.

Future research should explore scaling the proposed models to diverse domains and fine-tuning existing time series foundation models (e.g., Timer [24], Chronos [1]) to enable adaptation to arbitrary intervals, as presented herein. Furthermore, a theoretical analysis, potentially leveraging PAC-learning frameworks [34], to justify the performance disparity between the C-Policy and D_L^{*}-Policy offers a promising direction for future investigation and potential framework enhancements.

7 Acknowledgment

We thank Zhi-Quan (Tom) Luo for his insightful and constructive feedback, which significantly contributed to the development of this study. We also appreciate the assistance of Dachao Lin and Xi Zheng for their valuable help in providing and curating the wireless dataset used in this research.

⁷We provide additional results on the remaining datasets in the Appendix to support our claims.

Mod.	Train Strat.	\mathcal{I}_1	\mathcal{I}_2	\mathcal{I}_3	\mathcal{I}_4	\mathcal{I}_5	\mathcal{I}_6	\mathcal{I}_7	\mathcal{I}_8	Avg.
DLinear	D ₈ -Policy	167.1	76	56.7	44.2	33.5	28.1	19.3	11.1	54
	D ₁₆ ¹ -Policy	172.3	74.9	56	43.8	33.4	27.9	19.2	11.1	54.8
	D ₁₆ [∞] -Policy	164.9	75.7	56.7	44.4	33.8	28.2	19.4	11.2	54.3
	B-Policy	163.8	82.4	62	48.9	37.6	31.8	21.7	12.5	57.6
	C _{0.1} -Policy	218	84.8	58.8	43.4	31.7	26.4	18.8	10.9	61.6
	Improvement	0.0%	9.1%	9.7%	11.2%	15.7%	16.9%	13.4%	12.8%	6.3%
TimeMixer	D ₈ -Policy	127.5	40.1	24.3	16.1	10.8	8	5.5	3.3	29.4
	D ₁₆ ¹ -Policy	148.1	37.8	22.9	15.4	10.2	7.8	5.5	3.5	31.4
	D ₁₆ [∞] -Policy	138	41.7	23.8	15.8	10.4	8	5.6	3.4	30.9
	B-Policy	125.9	83	64.9	48.1	35.8	30.2	21.8	12.1	52.7
	C _{0.1} -Policy	143.7	50.7	32	20.8	13.1	9.3	6.1	3.6	34.9
	Improvement	0.0%	54.5%	64.7%	68.0%	71.5%	74.2%	74.8%	72.7%	44.2%
iTransformer	D ₈ -Policy	119.3	74.7	57.1	44	31.4	25.2	19.2	11.2	47.8
	D ₁₆ ¹ -Policy	121.1	75.9	58.4	44.6	32.1	25.7	19.5	11.2	48.6
	D ₁₆ [∞] -Policy	122.8	75.7	57.6	44.1	31.9	25.7	19.5	11.2	48.6
	B-Policy	130.8	77.3	59.5	46.8	35.5	29.8	20.6	11.8	51.5
	C _{0.1} -Policy	133.1	75.6	56	42.1	28.7	23.3	18.1	11.4	48.5
	Improvement	8.8%	3.4%	5.9%	10.0%	19.2%	21.8%	12.1%	5.1%	7.2%
PatchTST	D ₈ -Policy	102.8	31.1	18.3	11.4	7.1	4.5	2.7	1.7	22.4
	D ₁₆ ¹ -Policy	158.2	30.4	17.2	10.4	6.5	4	2.4	1.5	28.8
	D ₁₆ [∞] -Policy	117.8	35.3	20.8	12.6	7.9	5	2.8	1.8	25.5
	B-Policy	124.1	77.9	60.3	47.2	34.9	29.4	20.4	11.7	50.7
	C _{0.1} -Policy	118.1	34.6	22.5	15.2	9.8	6.8	3.9	2.6	26.7
	Improvement	17.2%	60.9%	71.5%	78.0%	81.4%	86.3%	88.2%	87.2%	55.8%

Table 2: MAE values ($\times 10^3$) for the four different models (DLinear, TimeMixer, iTransformer, and PatchTST) trained with the four policies (D₈-Policy, D₁₆¹-Policy, D₁₆[∞]-Policy, B-Policy, and C_{0.1}-Policy) on the BLW-TrafficDS trace. The highlighted values represent the lowest MAEs for a specific model in its respective column, while the underlined values represent the overall lowest MAEs for their respective columns. The improvement of a model is measured as a comparison between the best performing training policy and the baseline policy. The intervals of interest, denoted as $\mathcal{I}_1, \mathcal{I}_2, \dots, \mathcal{I}_8$, correspond to a partition of the time series range \mathcal{X} into eight contiguous sub-intervals of equal length.

References

- [1] Abdul Fatir Ansari, Lorenzo Stella, Caner Turkmen, Xiyuan Zhang, Pedro Mercado, Huibin Shen, Oleksandr Shchur, Syama Rangapuram, Sebastian Pineda Arango, Shubham Kapoor, et al. Chronos: Learning the language of time series. 2024.
- [2] Yoshua Bengio. Using a financial training criterion rather than a prediction criterion. *International journal of neural systems*, 8(04):433–443, 1997.
- [3] Christoph Bergmeir, Frits de Nijs, Abishek Sriramulu, Mahdi Abolghasemi, Richard Bean, John Betts, Quang Bui, Nam Trong Dinh, Nils Einecke, Rasul Esmaeilbeigi, et al. Comparison and evaluation of methods for a predict+optimize problem in renewable energy. *arXiv preprint arXiv:2212.10723*, 2022.
- [4] Dimitris Bertsimas and Nathan Kallus. From predictive to prescriptive analytics. *Management Science*, 66(3):1025–1044, 2020.
- [5] Robert G Brown. *Exponential smoothing for predicting demand*. Little, 1956.
- [6] Caltrans. Pems traffic data. <http://pems.dot.ca.gov>, 2016.
- [7] Chao Chen, Karl Petty, Alexander Skabardonis, Pravin Varaiya, and Zhanfeng Jia. Freeway performance measurement system: mining loop detector data. *Transportation research record*, 1748(1):96–102, 2001.
- [8] Jiezhong Cheng, Kaizhu Huang, and Zibin Zheng. Fitting imbalanced uncertainties in multi-output time series forecasting. *ACM Transactions on Knowledge Discovery from Data*, 17(7):1–23, 2023.
- [9] Ben Cohen, Emaad Khwaja, Kan Wang, Charles Masson, Elise Ramé, Youssef Doubli, and Othmane Abou-Amal. Toto: Time series optimized transformer for observability. *arXiv preprint arXiv:2407.07874*, 2024.
- [10] Abhimanyu Das, Weihao Kong, Rajat Sen, and Yichen Zhou. A decoder-only foundation model for time-series forecasting. In *Forty-first International Conference on Machine Learning*, 2024.
- [11] Adam N Elmachtoub and Paul Grigas. Smart “predict, then optimize”. *Management Science*, 68(1):9–26, 2022.
- [12] Marzyeh Ghassemi, Marco Pimentel, Tristan Naumann, Thomas Brennan, David Clifton, Peter Szolovits, and Mengling Feng. A multivariate timeseries modeling approach to severity of illness assessment and forecasting in icu with sparse, heterogeneous clinical data. In *Proceedings of the AAAI conference on artificial intelligence*, volume 29, 2015.
- [13] Mononito Goswami, Konrad Szafer, Arjun Choudhry, Yifu Cai, Shuo Li, and Artur Dubrawski. Moment: A family of open time-series foundation models. *arXiv preprint arXiv:2402.03885*, 2024.
- [14] Josif Grabocka, Randolph Scholz, and Lars Schmidt-Thieme. Learning surrogate losses. *arXiv preprint arXiv:1905.10108*, 2019.
- [15] Clive William John Granger and Paul Newbold. *Forecasting economic time series*. Academic press, 2014.
- [16] Yangdong He and Jiabao Zhao. Temporal convolutional networks for anomaly detection in time series. In *Journal of Physics: Conference Series*, volume 1213, page 042050. IOP Publishing, 2019.
- [17] Ignacio Hounie, Javier Porras-Valenzuela, and Alejandro Ribeiro. Loss shaping constraints for long-term time series forecasting. In *Proceedings of the 41st International Conference on Machine Learning*, pages 19062–19084, 2024.
- [18] Rob J Hyndman and George Athanasopoulos. 8.9 seasonal arima models. *Forecasting: principles and practice. oTexts. Retrieved*, 19, 2015.
- [19] S Levine, C Finn, T Darrell, and P Abbeel. End-to-end training of deep visuomotor policies. *arxiv*. URL: <https://arxiv.org/abs/1504.00702>, 2016.
- [20] Na Li, Donald M Arnold, Douglas G Down, Rebecca Barty, John Blake, Fei Chiang, Tom Courtney, Marianne Waito, Rick Trifunov, and Nancy M Heddle. From demand forecasting to inventory ordering decisions for red blood cells through integrating machine learning, statistical modeling, and inventory optimization. *Transfusion*, 62(1):87–99, 2022.
- [21] Yong Liu, Tengge Hu, Haoran Zhang, Haixu Wu, Shiyu Wang, Lintao Ma, and Mingsheng Long. itransformer: Inverted transformers are effective for time series forecasting. *arXiv preprint arXiv:2310.06625*, 2023.
- [22] Yong Liu, Tengge Hu, Haoran Zhang, Haixu Wu, Shiyu Wang, Lintao Ma, and Mingsheng Long. itransformer: Inverted transformers are effective for time series forecasting, 2024.
- [23] Yong Liu, Haixu Wu, Jianmin Wang, and Mingsheng Long. Non-stationary transformers: Exploring the stationarity in time series forecasting. *Advances in neural information processing systems*, 35:9881–9893, 2022.

- [24] Yong Liu, Haoran Zhang, Chenyu Li, Xiangdong Huang, Jianmin Wang, and Mingsheng Long. Timer: Transformers for time series analysis at scale. *arXiv e-prints*, pages arXiv–2402, 2024.
- [25] Ilya Loshchilov and Frank Hutter. Decoupled weight decay regularization. *arXiv preprint arXiv:1711.05101*, 2017.
- [26] Luis Martín, Luis F Zarzalejo, Jesus Polo, Ana Navarro, Ruth Marchante, and Marco Cony. Prediction of global solar irradiance based on time series analysis: Application to solar thermal power plants energy production planning. *Solar Energy*, 84(10):1772–1781, 2010.
- [27] Yuqi Nie, Nam H Nguyen, Phanwadee Sinthong, and Jayant Kalagnanam. A time series is worth 64 words: Long-term forecasting with transformers. *arXiv preprint arXiv:2211.14730*, 2022.
- [28] Yuqi Nie, Nam H. Nguyen, Phanwadee Sinthong, and Jayant Kalagnanam. A time series is worth 64 words: Long-term forecasting with transformers, 2023.
- [29] Junwoo Park, Jungsoo Lee, Youngin Cho, Woncheol Shin, Dongmin Kim, Jaegul Choo, and Edward Choi. Deep imbalanced time-series forecasting via local discrepancy density. In *Joint European Conference on Machine Learning and Knowledge Discovery in Databases*, pages 139–155. Springer, 2023.
- [30] Meng Qi, Yuanyuan Shi, Yongzhi Qi, Chenxin Ma, Rong Yuan, Di Wu, and Zuo-Jun Shen. A practical end-to-end inventory management model with deep learning. *Management Science*, 69(2):759–773, 2023.
- [31] Zheng Qian, Yan Pei, Hamidreza Zareipour, and Niya Chen. A review and discussion of decomposition-based hybrid models for wind energy forecasting applications. *Applied energy*, 235:939–953, 2019.
- [32] Evan L Ray, Yijin Wang, Russell D Wolfinger, and Nicholas G Reich. Flusion: Integrating multiple data sources for accurate influenza predictions. *Epidemics*, 50:100810, 2025.
- [33] UCI Machine Learning Repository. Electricityloaddiagrams20112014. <https://archive.ics.uci.edu/ml/datasets/ElectricityLoadDiagrams20112014>, 2014.
- [34] Shai Shalev-Shwartz and Shai Ben-David. *Understanding machine learning: From theory to algorithms*. Cambridge university press, 2014.
- [35] Sima Siami-Namini, Neda Tavakoli, and Akbar Siami Namin. The performance of lstm and bilstm in forecasting time series. In *2019 IEEE International conference on big data (Big Data)*, pages 3285–3292. IEEE, 2019.
- [36] Kai Wang, Boris Babenko, and Serge Belongie. End-to-end scene text recognition. In *2011 International conference on computer vision*, pages 1457–1464. IEEE, 2011.
- [37] Shiyu Wang, Haixu Wu, Xiaoming Shi, Tengge Hu, Huakun Luo, Lintao Ma, James Y. Zhang, and Jun Zhou. Timemixer: Decomposable multiscale mixing for time series forecasting, 2024.
- [38] Gerald Woo, Chenghao Liu, Akshat Kumar, Caiming Xiong, Silvio Savarese, and Doyen Sahoo. Unified training of universal time series forecasting transformers. 2024.
- [39] Haixu Wu, Jiehui Xu, Jianmin Wang, and Mingsheng Long. Autoformer: Decomposition transformers with auto-correlation for long-term series forecasting. *Advances in neural information processing systems*, 34:22419–22430, 2021.
- [40] Haixu Wu, Hang Zhou, Mingsheng Long, and Jianmin Wang. Interpretable weather forecasting for worldwide stations with a unified deep model. *Nature Machine Intelligence*, 5(6):602–611, 2023.
- [41] Wang Xue, Tian Zhou, Qingsong Wen, Jinyang Gao, Bolin Ding, and Rong Jin. Card: Channel aligned robust blend transformer for time series forecasting. *arXiv preprint arXiv:2305.12095*, 2023.
- [42] Ailing Zeng, Muxi Chen, Lei Zhang, and Qiang Xu. Are transformers effective for time series forecasting? In *Proceedings of the AAAI conference on artificial intelligence*, volume 37, pages 11121–11128, 2023.
- [43] Jun Zhang and Kim-Fung Man. Time series prediction using rnn in multi-dimension embedding phase space. In *SMC’98 conference proceedings. 1998 IEEE international conference on systems, man, and cybernetics (cat. no. 98CH36218)*, volume 2, pages 1868–1873. IEEE, 1998.
- [44] Yunhao Zhang and Junchi Yan. Crossformer: Transformer utilizing cross-dimension dependency for multivariate time series forecasting. In *The eleventh international conference on learning representations*, 2023.
- [45] Haoyi Zhou, Shanghang Zhang, Jieqi Peng, Shuai Zhang, Jianxin Li, Hui Xiong, and Wancai Zhang. Informer: Beyond efficient transformer for long sequence time-series forecasting. In *Proceedings of the AAAI conference on artificial intelligence*, volume 35, pages 11106–11115, 2021.
- [46] Tian Zhou, Ziqing Ma, Qingsong Wen, Xue Wang, Liang Sun, and Rong Jin. Fedformer: Frequency enhanced decomposed transformer for long-term series forecasting. In *International conference on machine learning*, pages 27268–27286. PMLR, 2022.

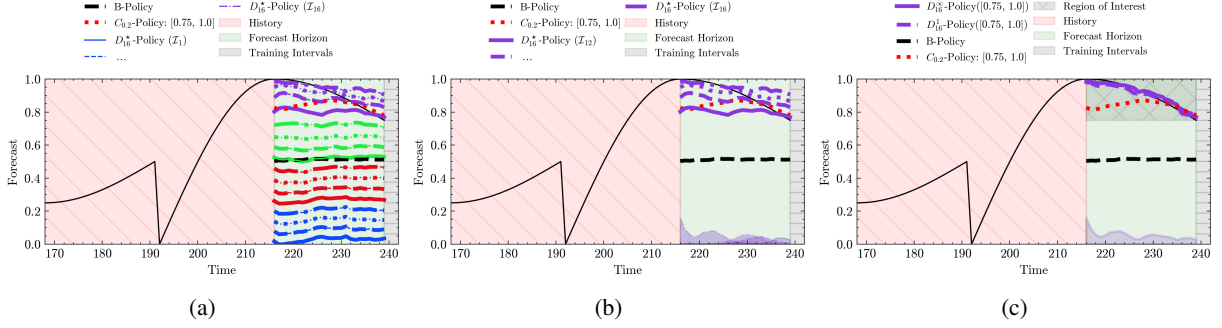


Figure 5: Forecasting results on a noiseless SynthDS trace. (a) Forecasts generated by the three policies: B-Policy, C-Policy, and D_L^* -Policy. (b) Isolated forecasts for the training intervals that cover the target interval of interest, $\mathcal{I} = [0.75, 1.0]$. This subfigure also illustrates the probability distribution over training intervals in $\Xi_{16}(\mathcal{I})$ from which a forecast is drawn. (c) Final forecast produced by D_L^* -Policy using patching strategies $\star \in \{1, \infty\}$. The B-Policy aggregates predictions and averages hypotheses centered around 0.5 (see Figure 3a), and consequently fails to capture distinct underlying signals. The C-Policy, trained on continuous intervals with minimum separation $\delta = 0.2$ and tuned for \mathcal{I} at inference time, better captures the signal in the target region, however with noticeable noise. In contrast, the D_L^* -Policy ($L = 16$), trained on L disjoint intervals, generates more discriminative forecasts with improved alignment to the true signal within \mathcal{I} . Although forecasts beyond the trained intervals remain noisy, interval classification facilitates identification of trustworthy predictions, enabling more accurate forecast patching during inference. D_L^* -Policy refines this process further by combining probabilistic interval classification with overlapping interval training, allowing the model to adaptively concentrate on relevant regions during inference.

A Additional Experiments

Discussion on Additional Experiments. Our evaluation of training policies on the Traffic, Weather, and Electricity datasets in Table 3 reveals consistent trends with our earlier findings on the SynthDS and BLW-TrafficDS traces. Specifically, the B-Policy consistently gives the poorest performance. The C-Policy offers modest improvements, suggesting that focusing on specific intervals during training provides performance improvement. The D_L -Policy, configured with the exact inference-time intervals achieves the best results. Incorporating patching through the D_L^* -Policy introduces a slight degradation in some cases, yet it often maintains or even improves overall MAE—due to an ensemble effect. We also observe that there are instances where patching slightly underperforms compared to the optimally tuned D_L -Policy, it is important to note that such prior knowledge of interval boundaries is rarely available in practice. Therefore, the D_L^* -Policy offers a more practical and robust alternative, consistently outperforming both the C-Policy and the B-Policy across most scenarios.

Figure 5 presents a simplified visual comparison of different forecasting policies on a noiseless version of the SynthDS dataset, where the only source of variability is from the random selection among four distinct underlying signals (Figure 3a). The B-Policy aggregates predictions across these hypotheses, producing forecasts centered around 0.5 and thereby failing to capture the underlying signals. The C-Policy, trained on continuous intervals with a minimum separation of $\delta = 0.2$ and tuned for the interval of interest \mathcal{I} at inference time, demonstrates improved tracking of the target signal but exhibits residual noise. In contrast, the D_L^* -Policy ($L = 16$), trained on L disjoint intervals, produces more discriminative forecasts with enhanced alignment to the ground truth within \mathcal{I} . While predictions outside the trained intervals remain noisy, interval classification enables the model to identify reliable forecasts, supporting more accurate patching at inference time. This process is further refined through Interval-Based Forecast Patching, which integrates probabilistic interval classification with overlapping interval training to allow for adaptive, region-specific focus during inference.

Mod.	Train Strat.	\mathcal{I}_1	\mathcal{I}_2	\mathcal{I}_3	\mathcal{I}_4	Avg.	Mod.	Train Strat.	\mathcal{I}_1	\mathcal{I}_2	\mathcal{I}_3	\mathcal{I}_4	Avg.
Traffic Dataset (MAE $\times 500$)													
DLinear	D ₄ -Policy	1.70	1.65	0.61	0.45	1.10	TimeMixer	D ₄ -Policy	1.90	1.25	0.39	0.22	0.94
	D ₈ ¹ -Policy	1.53	1.35	0.44	0.31	0.90		D ₈ ¹ -Policy	1.71	1.23	0.36	0.20	0.88
	D ₈ [∞] -Policy	1.67	1.44	0.47	0.33	0.98		D ₈ [∞] -Policy	1.73	1.27	0.41	0.24	0.91
	B-Policy	1.79	1.99	0.81	0.59	1.29		B-Policy	2.44	2.02	0.74	0.59	1.45
	C _{0.2} -Policy	1.82	1.71	0.62	0.45	1.15		C _{0.2} -Policy	2.17	1.52	0.51	0.35	1.14
Improvement		14.5%	32.2%	45.7%	47.5%	30.2%	Improvement		29.9%	39.2%	51.5%	66.2%	39.3%
PatchTST	D ₄ -Policy	1.08	0.91	0.32	0.16	0.62	iTransformer	D ₄ -Policy	1.29	1.19	0.53	0.35	0.84
	D ₈ ¹ -Policy	1.02	0.90	0.30	0.16	0.59		D ₈ ¹ -Policy	1.30	1.22	0.54	0.36	0.85
	D ₈ [∞] -Policy	1.06	0.93	0.35	0.19	0.63		D ₈ [∞] -Policy	1.32	1.24	0.55	0.37	0.87
	B-Policy	1.41	1.42	0.65	0.53	1.01		B-Policy	1.41	1.50	0.66	0.51	1.02
	C _{0.2} -Policy	1.11	0.89	0.30	0.16	0.62		C _{0.2} -Policy	1.36	1.13	0.53	0.35	0.84
Improvement		27.7%	37.3%	53.9%	69.8%	41.6%	Improvement		8.5%	20.7%	19.7%	31.4%	17.6%
Weather Dataset (MAE $\times 2$)													
DLinear	D ₄ -Policy	1.05	0.36	0.13	0.16	0.43	TimeMixer	D ₄ -Policy	2.25	0.37	0.19	0.17	0.75
	D ₈ ¹ -Policy	0.76	0.23	0.09	0.14	0.31		D ₈ ¹ -Policy	0.73	0.22	0.08	0.12	0.29
	D ₈ [∞] -Policy	0.75	0.29	0.10	0.21	0.34		D ₈ [∞] -Policy	0.71	0.26	0.09	0.13	0.30
	B-Policy	0.78	0.42	0.20	0.21	0.40		B-Policy	1.00	0.54	0.26	0.27	0.52
	C _{0.2} -Policy	1.32	0.36	0.26	0.27	0.55		C _{0.2} -Policy	1.94	0.43	0.25	0.26	0.72
Improvement		3.9%	45.2%	55.0%	33.3%	22.5%	Improvement		27.0%	59.3%	69.2%	55.6%	44.2%
PatchTST	D ₄ -Policy	0.40	0.22	0.08	0.10	0.20	iTransformer	D ₄ -Policy	0.49	0.32	0.18	0.19	0.30
	D ₈ ¹ -Policy	0.67	0.23	0.09	0.13	0.28		D ₈ ¹ -Policy	0.48	0.32	0.17	0.19	0.29
	D ₈ [∞] -Policy	0.53	0.28	0.11	0.14	0.26		D ₈ [∞] -Policy	0.49	0.32	0.18	0.19	0.29
	B-Policy	0.65	0.37	0.22	0.23	0.37		B-Policy	0.68	0.42	0.23	0.21	0.38
	C _{0.2} -Policy	1.17	0.22	0.08	0.11	0.40		C _{0.2} -Policy	1.72	0.49	0.39	0.38	0.74
Improvement		38.5%	40.5%	63.6%	56.5%	46.0%	Improvement		29.4%	23.8%	26.1%	9.5%	23.7%
Electricity Dataset (MAE $\times 10^{-1}$)													
DLinear	D ₄ -Policy	3.809	1.148	0.916	0.369	1.560	TimeMixer	D ₄ -Policy	3.828	1.112	0.807	0.297	1.511
	D ₈ ¹ -Policy	3.815	1.156	0.929	0.379	1.570		D ₈ ¹ -Policy	3.946	1.070	0.782	0.277	1.519
	D ₈ [∞] -Policy	3.820	1.159	0.932	0.380	1.572		D ₈ [∞] -Policy	3.953	1.087	0.836	0.288	1.541
	B-Policy	3.767	1.165	0.955	0.399	1.571		B-Policy	4.498	1.412	1.081	0.449	1.860
	C _{0.2} -Policy	3.947	1.139	0.890	0.353	1.582		C _{0.2} -Policy	4.863	1.369	0.984	0.388	1.901
Improvement		0%	2.23%	6.81%	7.52%	0.70%	Improvement		14.90%	24.29%	27.65%	38.31%	18.75%
PatchTST	D ₄ -Policy	3.332	0.919	0.671	0.238	1.290	iTransformer	D ₄ -Policy	12.750	4.668	2.077	0.567	5.016
	D ₈ ¹ -Policy	4.664	1.243	0.852	0.248	1.752		D ₈ ¹ -Policy	10.311	3.693	1.843	0.509	4.089
	D ₈ [∞] -Policy	4.689	1.338	0.931	0.272	1.808		D ₈ [∞] -Policy	10.504	3.835	1.982	0.522	4.211
	B-Policy	3.324	1.014	0.835	0.370	1.386		B-Policy	3.259	1.050	0.861	0.372	1.386
	C _{0.2} -Policy	3.778	0.990	0.689	0.243	1.425		C _{0.2} -Policy	3.668	1.024	0.822	0.322	1.459
Improvement		0%	9.37%	19.64%	35.68%	6.93%	Improvement		0%	2.48%	4.53%	13.44%	0%
Noiseless SynthDS Dataset (MAE $\times 100$)													
DLinear	D ₄ -Policy	10.73	11.33	14.38	16.48	13.23	TimeMixer	D ₄ -Policy	7.74	10.79	8.63	8.02	8.79
	D ₈ ¹ -Policy	13.06	13.29	14.18	17.96	14.62		D ₈ ¹ -Policy	12.57	12.89	11.69	13.44	12.65
	D ₈ [∞] -Policy	11.36	11.80	15.17	14.44	13.19		D ₈ [∞] -Policy	11.23	12.58	13.09	12.95	12.46
	B-Policy	56.97	16.05	12.74	52.58	34.58		B-Policy	33.61	28.24	25.97	32.94	30.19
	C _{0.2} -Policy	34.62	14.44	11.84	29.63	22.63		C _{0.2} -Policy	22.16	13.58	9.78	16.76	15.57
Improvement		81.2%	29.4%	7.06%	72.5%	61.8%	Improvement		77.0%	61.8%	66.8%	75.6%	70.9%
PatchTST	D ₄ -Policy	3.71	2.73	2.13	7.20	3.94	iTransformer	D ₄ -Policy	5.65	3.16	2.10	6.98	4.47
	D ₈ ¹ -Policy	7.35	6.71	6.93	7.16	7.04		D ₈ ¹ -Policy	5.73	3.17	3.81	7.18	4.97
	D ₈ [∞] -Policy	5.16	5.90	7.72	5.35	6.03		D ₈ [∞] -Policy	6.49	4.10	3.66	6.25	5.13
	B-Policy	18.05	28.37	23.28	32.16	25.47		B-Policy	19.16	28.17	25.22	25.87	24.60
	C _{0.2} -Policy	14.62	5.86	5.87	13.72	10.02		C _{0.2} -Policy	21.15	6.10	2.29	19.39	12.23
Improvement		79.4%	90.4%	90.9%	77.6%	84.5%	Improvement		70.5%	88.8%	91.7%	72.2%	81.8%

Table 3: The MAE values ($\times 500$ for Traffic, $\times 2$ for Weather, $\times 10^{-1}$ for Electricity, and $\times 100$ for Noiseless SynthDS) are reported for the four different models: DLinear, TimeMixer, iTransformer, and PatchTST. These models were trained using five distinct policies: D₄-Policy, D₈¹-Policy, D₈[∞]-Policy, B-Policy, and C_{0.2}-Policy on the Traffic, Weather, Electricity, and Noiseless SynthDS traces. Highlighted values indicate the lowest MAEs for each specific model within its respective column, while underlined values indicate the overall lowest MAEs across all models for each column. Model improvement is assessed by comparing the best-performing training policy against the baseline policy. The intervals of interest, denoted as $\mathcal{I}_1, \mathcal{I}_2, \dots, \mathcal{I}_4$, represent a partition of the time series domain \mathcal{X} into four contiguous sub-intervals of equal length.